INSTITUTE OF PHYSICS PUBLISHING MEASUREMENT SCIENCE AND TECHNOLOGY

Meas. Sci. Technol. **17** (2006) 3102–3109 doi:10.1088/0957-0233/17/11/031

Determination of the olfactory threshold using a piezoelectric microdispenser for neurodegenerative disease diagnostics

David B Wallace[1], David Taylor[1], Bogdan V Antohe[1], Ioan Achiriloaie[1], Norman Comparini[1], R Malcolm Stewart[2] and Manjit K Sanghera[2]

[1] MicroFab Technologies, Inc, Plano, TX, USA
[2] Human Performance Laboratory, Fogelson Neuroscience Center, Presbyterian Hospital of Dallas, Dallas, TX, USA

Received 5 April 2006, in final form 6 September 2006
Published 19 October 2006
Online at stacks.iop.org/MST/17/3102

Abstract
Ink-jet microdispensing technology was used to develop an instrument for the quantitative determination of the olfactory threshold. An electrical pulse applied to the piezoelectric element produces a deformation that is transmitted to the fluid which results in a drop of fluid being ejected through the orifice mounted at one end of a piezoelectric tube. An electronic console actuates the piezoelectric dispensing elements and controls the number of drops that are dispensed and evaporated to create a fragrance cloud. The number of drops that are generated, evaporated and presented to the patient's nose for detection is adjusted according to a preset algorithm until the patient's threshold is discovered. Neurodegenerative disease patients tested with the developed olfactometer showed a significant elevation of their olfactory threshold as compared to normal controls. This result agrees with literature studies that indicate the sense of smell is one of the first affected by neurodegenerative disease. Through its precise control and detection capability, the digital olfactometer described in this paper can be used as an early screening tool for neurodegenerative disease through olfactory threshold determination.

Keywords: olfaction, threshold, diagnostics, neurodegenerative disease, ink-jet, microdispensing

Nomenclature

c_p	specific heat of air (kJ kg^{-1} °C^{-1})
D	mass diffusion coefficient of phenethyl alcohol vapours in air (m^2 s^{-1})
d	diameter (m)
h	heat or mass transfer coefficient
Le	Lewis number $Le = \frac{\alpha}{D}$
l	length of the annular piezoelectric transducer (m)
L	representative length for Reynolds number (m)
m''	evaporation flux (kg m^{-2} s^{-1})
$\dot{m}$	evaporation rate (kg s^{-1})
Pr	Prandtl number $Pr = \frac{\nu}{\alpha}$
Re	Reynolds number $Re = \frac{uL}{\nu}$
u	airstream velocity (m s^{-1})

Greek letters

α	thermal diffusivity of air (m^2 s^{-1})
ν	kinematic viscosity of air (m^2 s^{-1})
ρ	air density (kg m^{-3})

Subscripts

1	outer surface of the tube
2	inner surface of the tube
c	heat convection
m	mass convection
orif	orifice
sat	saturated
vap	referring to the vapours of phenethyl alcohol

1. Introduction

A study of the US population based on the 2000 Census reports that 4.5 million had Alzheimer's disease, and the prevalence (the number of people with the disease at any one time) is expected to at least double by 2050 for every 5 year age group beyond age 65 [1]. Nearly half of all people aged 85 or older currently have Alzheimer's disease. Researchers estimate that by 2050, 13.2 million Americans will have Alzheimer's disease if no preventive treatments become available [1]. With advancements in physical and mental health care more Americans will be reaching older ages. As the number of individuals 85 years of age or older increases so will the number of Alzheimer's cases.

The annual cost of caring for an Alzheimer's disease patient depends upon the severity of the disease with a total estimated direct and indirect annual cost of care for Alzheimer's disease patients of $100 billion. The cost and the implications of the disease on the caregivers and families make early detection and diagnosis of neurogenerative disease and especially Alzheimer's disease a high priority. Early diagnosis followed by interventions that could delay the onset of the disease or slow down its progress would significantly aid the caregivers and reduce the cost of care.

Several areas have been explored to improve the ability to identify the initial symptoms of neurodegeneration. These tests are based on detecting and quantifying cognitive changes that occur in the brain of a person with Alzheimer's or other neurodegenerative diseases. Examples include neuropsychological diagnostic tests that measure delayed recall, verbal fluency and overall cognitive status.

A comparison study between a group of probable Alzheimer's patients and a group of aged matched adults analysed if the volumetric measures of mesial temporal region of the brain that take part in the processing of the olfaction information is related to the performance in the olfaction tests including odour identification and olfaction threshold [2]. The investigators found a strong correlation between the sense and smell and the hippocampal volume and indicated the potential clinical utility of odour identification tests for detecting Alzheimer's disease.

Further studies indicated that, in its initial stages, Alzheimer's disease attacks medial temporal lobe structures that are critical in smell identification [3, 4]. As the disease progresses, further deficits appear in the patient's ability to identify and detect odours, and awareness of the deficit [5–7]. To establish the use of olfaction as a diagnostics tool for neurological diseases, significant efforts were made to create correlations between olfaction and other testing methods and between olfaction and other symptoms of the neourodegenerative disease [8, 9].

A method capable of quantifying the patients' olfactory capability will not only facilitate early diagnosis of neurodegenerative diseases such as Alzheimer's or Parkinson's, but will also provide the means to track the progression of the disease [10, 11]. However, the means to make an accurate and reliable assessment of a patient based on the olfactory threshold remains a challenge [12, 13]. Disease progression as a clinical tool has been problematic due to the complexity of administering specific concentrations and varieties of odorants to a patient in a controlled manner. This complexity has often meant reliance on complex and expensive research olfactometers. Conversely, scratch-and-sniff tests, while cost efficient and widely used, are neither versatile in their testing modality nor consistent in their odorant composition from year to year.

The University of Pennsylvania Smell Identification Test (UPSIT) is the most widely used scratch-and-sniff test for determining smell identification deficits [14]. This test uses odorants sequestered in microencapsulated crystals that release the odorant when scratched. During the test, the patient selects the odorant out of four given choices. Although the precise amount of odorant released from the crystals upon scratching has not been determined, the test has proven successful in identifying and discriminating smell identification deficits in a number of neurodegenerative disorders [15]. However, this scratch-and-sniff test does not enable quantification of the olfactory threshold. Other test systems that focus on quantification are either very complex or require the manual handling of solutions of different concentrations [16–18].

The olfactometer technology described in this paper is based on digitally controlled, high precision ink-jet dispensing technology and is capable of determining the olfactory threshold. The threshold for specific odorants is determined to a very high-resolution because ink-jet microdispensers are capable of delivering nanomolar quantities of odorant per ejected drop. The system can dispense many odorants through the use of interchangeable cartridges. The resolution can be extended past single drop dispensing by using dilutions of the odorants used in the tests.

2. Olfactometer design

The digital olfactometer (figure 1) consists of four piezoelectric ink-jet microdispenser modules—each module is used for a different odorant or odorant dilution—placed two on each side of a heating element in a 'V' configuration (figure 2) [19, 20]. Each microdispenser module is composed of a piezoelectric dispenser with a reservoir and electrical connections for the actuating signal. The olfactometer is connected electrically to a control unit that selects the dispenser and number of drops of the corresponding odorant to be dispensed. The drops are dispensed onto the heating element and the odorant vapour cloud is presented to the patient's nose by a miniature fan. The main parts of the system (figure 2) are discussed below.

2.1. Microdispenser and reservoir module

The microdispenser is made of a piezoelectric element that has an electroformed orifice plate (orifice diameter $d_{\mathrm{orif}} = 45\ \mu$m) soldered at one end and is oriented towards the heating element. The other end is connected to the supply reservoir [21]. A stainless sleeve is bonded to the piezoelectric tube and C-flex tubing is inserted in the sleeve to seal against the capillary Teflon tubing used as a reservoir. To avoid dripping of the fluid through the orifice plate, the reservoir consists of 0.012″ (0.305 mm) ID capillary Teflon™ tubing. The capillary forces and the fact that the tubing is coiled with a small height

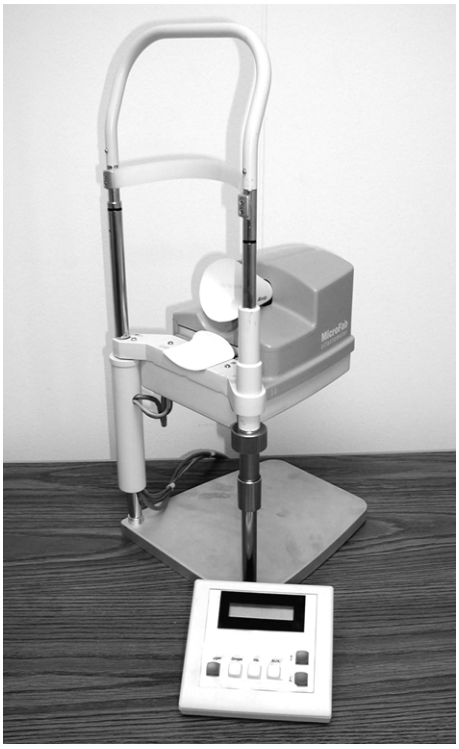

Figure 1. Olfactomer using ink-jet microdispensers and its control electronics console.

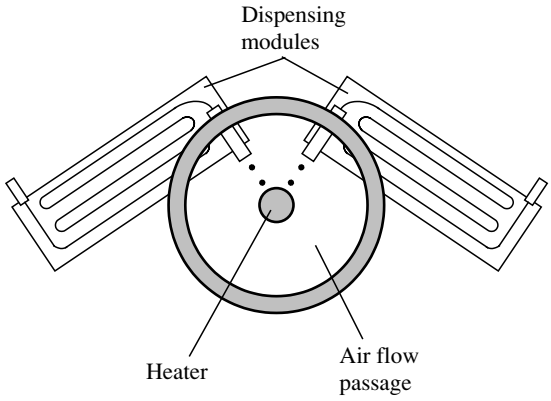

Figure 2. Diagram of the ink-jet based vapour generator component. The dispensing modules are placed in a V configuration such that the odorant droplets land on the centrally placed heater. Another pair of microdispenser modules is placed behind the one shown in the sketch for a total of four modules.

variation prevent the dripping of fluid through the orifice and reduce the pressure variations at the orifice level (figures 2 and 3). The length of the tubing corresponds to a volume of approximately 28 μl. A port at the end of the capillary tubing is used to refill the module.

The dispenser actuator is an annular PZT5A piezoelectric element, with a radial polarization direction. The dimensions of the piezoelectric tube are $d_1 = 0.070''$ (1.78 mm), $d_2 = 0.050''$ (1.27 mm) and $l = 0.6''$ (15.24 mm) (figure 4). Electrodes for actuation are deposited on both inner and outer surfaces. The inner electrode wraps around the tube end onto the outside surface of the tube for an easier electrical

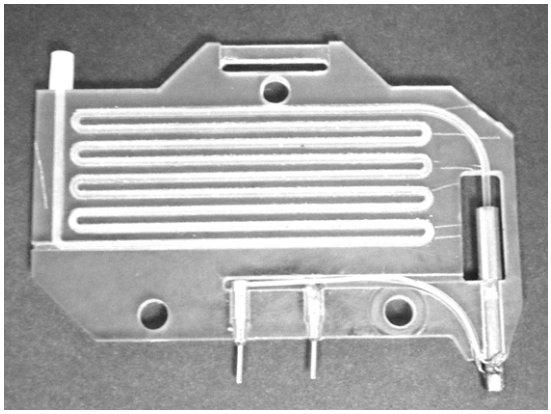

Figure 3. Microdispenser module. The reservoir is made of small capillary Teflon^{TM} tubing and is loaded with odorant through the top. Electrical contacts plug in a matching connector in the olfactometer that provides the electrical signal from the control console and the mechanical support.

connection. The metallic (nickel) plating was removed from the front of one end of the tube and from a section of the outer surface to separate the two electrodes. Wires are soldered to the electrodes next to the strip where the plating was removed and, at the other end, to the pins that plug into the olfactomer.

2.2. Electronics for drop control and drop generation

Drop generation follows the principles of drop-on-demand (DOD) piezoelectric ink-jet printers. Figure 5 presents the main steps in the drop formation sequence. The actuating electrical signal consists of a trapezoidal waveform ('rise', 'dwell'—constant voltage, 'fall' to initial voltage) and is applied to the outer electrode while the inner electrode is grounded. During the 'rise' period the inner surface of the piezoelectric tube moves outward and a negative pressure wave is generated and starts to move both to the supply and orifice ends. When the negative pressure wave reaches the orifice, the meniscus (liquid air interface) withdraws into the dispenser nozzle (figure 5, second photograph). At the supply end the negative wave reflects back as a positive pressure wave. The 'dwell' period (time at maximum/constant voltage) is selected such that the 'fall' of the drive signal starts when the reflected positive pressure wave reaches the middle of the tube. The voltage 'fall' period corresponds to a compression of the fluid (inward motion of the tube wall) and thus reinforces the reflected wave for a minimization of the required voltage at a constant drop velocity or the maximization of the drop velocity at the same applied voltage. As the positive pressure wave reaches the orifice it will start ejecting the fluid that forms the drop (figure 5, third photograph).

The olfactometer electronics were designed to produce the signal described above where the rise and fall times are very short (<1 μs) and the dwell time is set at 25 μs. The dwell voltage can be adjusted and preset in the electronics. Odorants in this study were dispensed at a maximum/constant voltage of 80 V. When more than one drop is generated, the generation frequency can be adjusted within the range 88–997 Hz.

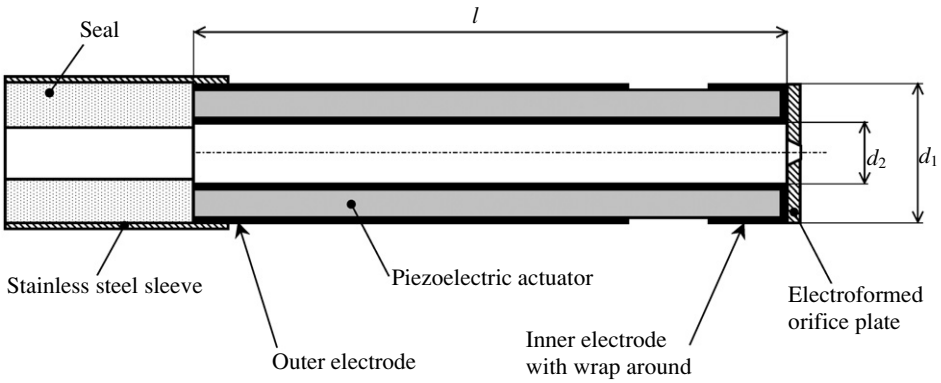

Figure 4. Dispenser construction. The capillary tubing is inserted in the sealing element at the back of the dispenser.

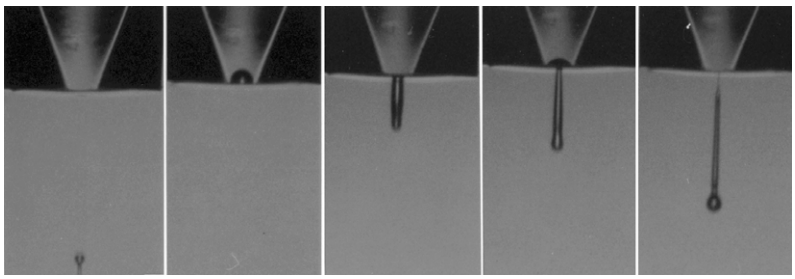

Figure 5. Drop ejection sequence at different instances during the drop formation process. The event is stroboscopically illuminated synchronized with the drop generation. By changing the delay between the signal applied to the piezoelectric actuator and the strobe delay, drops are 'frozen' at a specific state in the ejection sequence.

2.3. Vapour generation

In this study we used two odorants: phenethyl alcohol (PEA, Sigma Aldrich), that has a distinctive 'rose' smell, and a lemon extract (LE, McCormick). PEA was chosen because of its selectivity in stimulating the olfactory cranial nerve without affecting the intranasal trigeminal nerve endings and LE was included as a control because it is known to stimulate the trigeminal nerve [22]. Neither odorant is noxious.

The odorant begins as a liquid of known concentration that is loaded into the dispenser and capillary reservoir. The microdispenser is digitally controlled to produce one or more drops of precise volume, with each drop containing a fixed, discrete mass of the odorant. The drop size produced in these experiments was 94 pl. The microdispenser is rapidly triggered by a microprocessor to produce n drops containing a programmed mass of odorant representing the desired stimulus. Instantaneous odorant concentration changes can be pre-programmed or manually triggered over a 500:1 range. A push-button controller regulates the instrument functions and is used to step up and down between the different levels of number of drops used in the tests. The number of drops in the different trial levels is programmed to follow an exponential law (i.e. rounded to the closest integer: 1, 2, 3, 5, 6, 9, 12, 16, 21, 29, 39, 53, 73, 98, 134, 182, 257, 335, 455, 618, 839, 1139). This approach reduces the number of trials required for threshold determination.

Dispensed drops land on a heating element maintained at 200 °C, are heated to the 200 °C temperature and then evaporated in the air stream. A small fan is placed at the back of the air passage and its air flow carries the evaporated odorant plume to the patient's nose. The influence of the number of drops on the evaporated material is shown in figure 6 (the drops were generated at a frequency of 800 Hz). Here a ModuRAE PDM-10A photo ionization detector (PID) module (RAE Systems, Inc.) was used to measure the total volatile organic concentration of the vapour.

Table 1. Evaporation parameters as a function of the number of drops.

Number of drops	(a)	(b)	(c)
98	0.004	0.742	0.97
134	0.005	1.015	1.33
182	0.007	1.378	1.81
247	0.009	1.870	2.46
335	0.013	2.536	3.34
455	0.017	3.445	4.53
618	0.023	4.679	6.16
839	0.031	6.352	8.36
1139	0.042	8.623	11.35

Note: (a) Energy to heat up the fluid from 25 °C to 200 °C (J), (b) Energy to evaporate the fluid (J) and (c) Forced mass convection estimate of evaporation time (s).

The energy required to heat up the fluid from 25 °C to 200 °C and the energy required to evaporate the fluid were determined on the basis of the number of drops placed on the heater. These values are shown in table 1 where it can be observed that the vaporization energy is the dominant requirement for heating power.

When compared to the maximum heater power (6.6 W) which is determined by the heater resistance (100 Ω) and

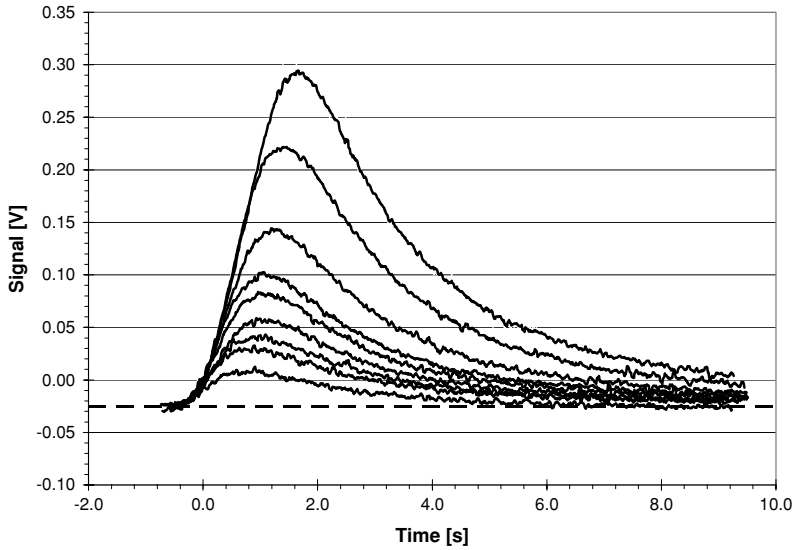

Figure 6. Odorant plume transient as a function of the number of dispensed drops. Curves are plotted for PEA dispensed at 800 Hz with the following number of drops: 98, 134, 182, 247, 335, 455, 618, 839, 1139. Curves are obtained using a photo ionization detector. The dotted line indicates the non-excited signal level of the sensor.

the applied voltage (25.7 V) these values are mostly lower. To deliver the energy required by the evaporation of the maximum number of drops (table 1) it would take 1.3 s which is shorter than the time (1.42 s) it takes for the 1139 drops to be dispensed at 800 Hz.

Previous evaporation studies showed that the time it takes a large drop (comparable to a collection of drops in our case) to heat up is small compared to the evaporation time [23]. We have estimated the evaporation time neglecting this initial warm up period. Estimates for the evaporation time can be determined by making use of the analogy between forced heat and mass transfer coefficients [24]:

$$h_{\mathrm{m}} = \frac{h_{\mathrm{c}}}{\rho\, c_{\mathrm{p}}\, Le^{2/3}}. \tag{1}$$

The Lewis number was estimated to be 3.9 using an average diffusivity (9×10^{-6} m^2 s^{-1}) of alcohols in air [25] because no data were found for phenethyl alcohol. Because the diffusivity data are at room temperature this results in an overevaluation of the Lewis number and an underevaluation of the mass transfer coefficient. The convection heat transfer coefficient was determined using the formula for the averaged forced convection along a flat plate [24]:

$$h_{\mathrm{c}} = 0.664 Pr^{1/3} Re^{1/2}. \tag{2}$$

Using the properties of the air at the film temperature (average temperature between the free air stream and the heater temperature) and the velocity of 0.3 m s^{-1}, the averaged forced convection heat transfer coefficient was found to be 15.03 W m^{-1} °C^{-1}. The corresponding mass transfer coefficient determined using equation (1) was 0.0065 kg m^{-2} s^{-1}.

The evaporation mass flux is determined by [23]

$$m'' = h_{\mathrm{m}}(\rho_{\mathrm{vap,sat}}(T) - \rho_{\mathrm{vap},\infty}), \tag{3}$$

where the saturated vapour density was considered at 200 °C temperature and the vapour density in the free stream was considered zero.

Assuming an average size (the mass transfer area decreases in time) of the mass transfer area to be of 0.5 mm radius the evaporation rate is $\dot{m} = 9.621 \times 10^{-9}$ kg s^{-1}. The total evaporation time of the liquid on the heater can be estimated by using the drop volume, number of drops and liquid density. The evaporation times as a function of number of drops are listed in the last column of table 1.

When comparing the estimates in table 1 with the sensor response it can be observed that the evaporation time estimates are shorter than the time it takes the sensor to return to the base voltage for the low number of drops. This is a result of the overestimation of the area for the mass transfer for the smaller number of drops. Other factors that could contribute to differences between the estimated evaporation time and the time shown by the PID module are the higher diffusivity (this leads to a smaller Lewis number that results in a larger mass transfer coefficient) at temperatures larger than 25 °C, the time it takes to dispense the specified number of drops (neglected in the estimation above), the time it takes for the heater to deliver the required evaporation energy, the time it takes for the sample to be drawn in and cleared out by the module and the sensor response time. The PID module has an internal pump that has a 400 cc min^{-1} flow rate which could result in up to half a second delay time. The response time of the sensor itself is reported by the manufacturer to be up to 3 s. Other factors that appear to be less significant [23] are the time it takes the droplets to reach the 200 °C temperature of the heater and possible local cooling effects of the heater.

Figure 7 presents the peak sensor signal (measured from the level of the unexcited sensor) and the time integral of the signal (area between the signal curve and the dotted line corresponding to the sensor not being excited) as a function of the number of drops. As expected, there is an almost linear relationship between the number of drops (proportional to the volume of odorant) and the integral value (representation of the amount of vapour generated). The integrals for larger volumes of odorants are underestimated as the concentration does not

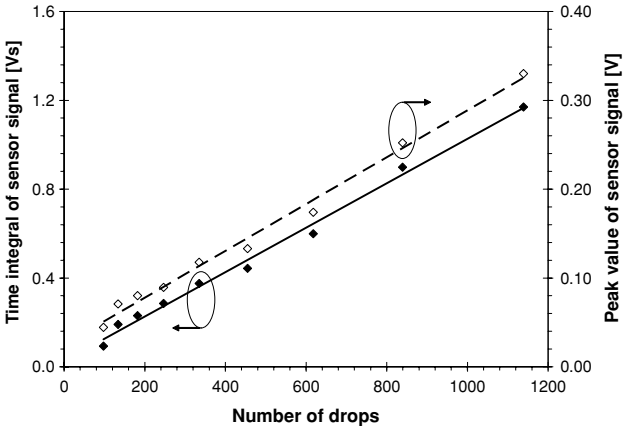

Figure 7. Correlation between the number of the odorant drops and the maximum sensor signal and the area under the signal curve.

return to the unexcited level in the time data were captured. From the figure it can also be observed that the peak signal value (representation of the maximum concentration) also varies almost linearly with the amount of odorant dispensed.

By using different frequencies for the same number of drops the curve appearance can be modified while maintaining the area between the curves and the *X* axis constant. The same number of drops (same total odorant amount) dispensed at a lower frequency will reduce the curve maximum and will extend the curve out in time (*X* axis). For this study we did not explore the frequency influence on the instantaneous output.

The repeatability of the olfactometer was evaluated in terms of the output. We have selected this approach rather than using the actual threshold of specific patients because the olfaction threshold can be affected by nasal discharge, allergies, illness and possibly by circadian rhythm [26]. The repeatability was evaluated by dispensing the same number of drops (839) over the heater and by comparing the peak values of the signals from the photo ionization detector. For 105 measurements we have determined that the peak value had a standard deviation of 7.6% from the maximum value (averaged over the total number of measurements).

3. Procedure for testing

All olfactory threshold testing was conducted in the Human Performance Laboratory at Presbyterian Hospital of Dallas in a well-ventilated room. The same test administrator ran all the testing reported in this paper.

3.1. Set-up

The odorants were loaded using sterile syringes into the reusable, sterilized cartridges. Several bursts of drops were ejected from each of the microdispensers to ensure priming. A new disposable paper nose cone used to direct the flow of the odorants was installed for each test subject. The test administrator gave the test subject the instructions regarding the procedure.

3.2. Testing

The testing followed a methodology that was used for tactile sensation tests [27]. For each trial within a test, discrete levels of odorants were presented to the subject's nose who was then asked to sniff on verbal cue and then provide a suitable response: 'yes' (odorant detected) or 'no' (odorant not detected). The test administrator interpreted the subject's responses and then adjusted the control stimulus intensity (number of drops) up or down depending on the subject's current and previous responses.

The starting level for the stimulation was set at 134 drops which was established in a previous study. This corresponds to 105 nanomoles for PE. Because the composition of the lemon extract was not known, it was not possible to calculate the corresponding number of moles. The first trial in a test establishes the stimulus level direction: 'down' for a 'yes' response, 'up' for a 'no' response. The test progresses similarly until a change in response pattern occurs (YYYN or NNNY). When such a change occurs, the next trial is conducted at the same level as the previous trial. For subsequent trials the direction of stimulus level is changed only when one of the following takes place:

(1) The subject does not detect the stimulus on two consecutive trials while moving to a lower concentration (YYYNN response pattern). In this case the following trial has the level set to the next higher level.
(2) The subject reports detection of the stimulus on two consecutive trials while moving up to a higher concentration (NNNYY response pattern). The following trial is performed at the next lower level.

A test is concluded when a third direction change occurs between the same two levels. The final estimate of the olfactory threshold is determined as the average of stimulus levels corresponding to the last two direction changes. The procedure described above is a modified staircase that was used in previous olfaction studies [28].

Figure 8 presents the individual trial results and the convergence towards the olfactory threshold for representative 'control' and 'smell deficient' patients. The control patient can detect smaller and smaller amounts of odorants until the detection/non-detection oscillates between two levels. The 'smell deficient' patient has a similar oscillatory behaviour between two levels that have a significantly higher amount than the starting level.

4. Test results

Healthy control candidates were recruited to cover a wide age range (approximately ten subjects per age decade from 20s through 80s) and to have a good representation of both males and females. All control candidates were administered the Folstein Mini-Mental Status Examination (MMSE) [29] to test for cognitive impairment as well as the clock drawing and clock copying tests to examine the integrity of frontal and parietal lobe function. To be included within the control group the test subjects had to have a MMSE score higher than 29, copy drawing and clock copying scores of 4/4 and to have (a) no family history of AD and/or PD, (b) no occurrence of any head trauma, (c) no decrease in memory, (d) no decrease in

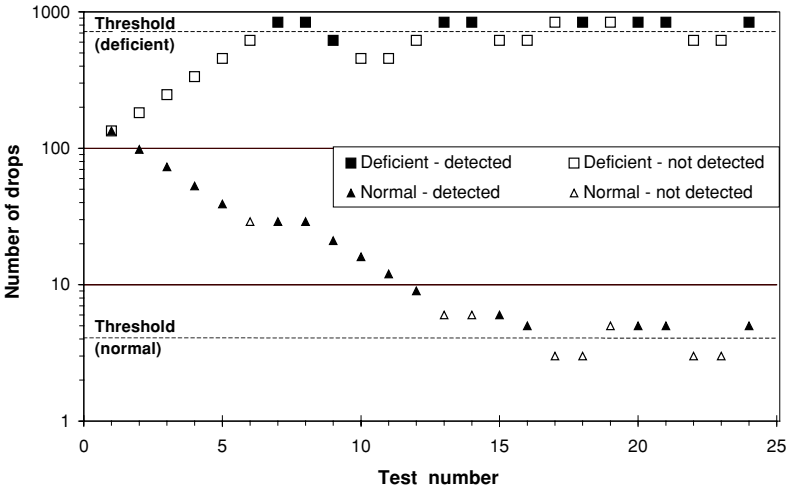

Figure 8. Example of threshold determination for normal and smell deficient patients established through a modified staircase algorithm.

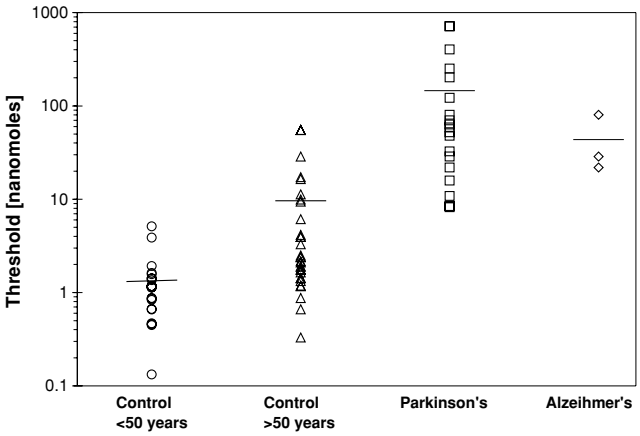

Figure 9. Comparison between the threshold for the control subjects and the Alzheimer's and Parkinson's patients. The horizontal lines indicate the arithmetic averages of the olfaction thresholds within each group of test subjects.

the ability to smell, (e) no presence of allergies and (f) had not smoked during the last 10 years. Alzheimer's and Parkinson's patients were recruited from the Neurology Outpatient Clinic at Presbyterian Hospital of Dallas (PHD).

Figure 9 summarizes the olfactory thresholds for control test subjects and patients diagnosed with Alzheimer's or Parkinson's. In the plot the control subjects were separated by age (younger and older than 50 years) to illustrate the age effects. The horizontal line drawn on the plot for each group indicates the average threshold for that specific group of test subjects.

5. Discussions

Healthy control subjects were able to learn the olfactory testing procedure quickly and they completed the test in approximately 20 min. For the PEA odorant (shown in figure 9), females and males <50 years were significantly different (lower thresholds, or more sensitive) from the corresponding >50 year old groups. Olfactory thresholds for both PEA and LE were generally lower in female control subjects as compared to male controls, although a significant difference was found only for PEA in the >50 year old group. Male control subjects displayed a greater variability in thresholds.

Significant differences were found between the Parkinson's patients and the healthy controls for both males and females. Even though there was some overlap in the threshold ranges for the >50 year old control group and the Parkinson's group, the average olfactory threshold for Parkinson's patients was higher than the highest olfactory threshold for the control groups.

For Alzheimer's disease patients (all five subjects were older than 50 years) we found significant differences when compared to the healthy controls. The Alzheimer's patients had very high thresholds. Attempts to determine accurately the olfactory thresholds were difficult, causing noticeable subject frustration and difficulty with keeping on task. Consequently, only two subjects were tested with both odorants.

6. Conclusions and future work

The objective of this study was to examine the operability of the prototype digital olfactometer in a test comparing the olfaction thresholds for a group of control patients with the olfaction thresholds for neurodegenerative disease patients. To our knowledge this is the first study where olfactory thresholds were measured in precise amounts by employing an ink-jet microdispenser for odorant dosage.

The olfactometer was able to detect differences between the control patients and the patients diagnosed with a neurodegenerative disease. The low end of the olfaction thresholds for neurodegenerative disease patients overlaps the high end of the thresholds for older control patients.

Other olfactory threshold trends were detected during the study. The olfactory threshold for both odorants was lower in female control subjects compared to male controls, although this difference was small. The results also indicated a trend of increasing threshold with age for both 'rose' and 'lemon'

in control subjects. The changes in the olfaction threshold in both males and females appeared to start around the 5th decade of life.

More experiments are necessary to better establish the correlation between the increase in the olfactory threshold and neurodegenerative disease. With the capability of precisely quantifying the threshold, the change in the olfaction threshold can be followed as the disease progresses. The digital olfactometer needs improvements to make the measurements easier and more precise. At issue was the synchronization between the patient's inhalation and the drop generation. An early inhalation could result in a false 'miss'. Improved versions of the olfactory instrument should incorporate a correlation between the inhalation and the drop generation and automation of the test and data acquisition.

Acknowledgments

The work presented in this paper was supported by NIH grant MH/DC56335. We acknowledge the support of the staff and patients at Presbyterian Hospital and the control group at Presbyterian Hospital and MicroFab Technologies, Inc. The authors are grateful to the referees for their careful review of this manuscript and their recommendations. The authors also thank Christian Rensch for collecting the data for the repeatability evaluations.

References

[1] Hebert L E, Scherr P A, Bienias J L, Bennett D A and Evans D A 2003 Alzheimer disease in the U.S. population: prevalence estimates using the 2000 census *Arch. Neurol.* **60** 1119–22

[2] Murphy C, Jernigan T L and Fennema-Notestine C 2003 Left hippocampal volume loss in Alzheimer's disease is reflected in performance on odor identification: a structural MRI study *J. Int. Neuropsychol. Soc* **9** 459–71

[3] Kesslak J P, Cotman C W, Chui H C, van Den Noort S, Fang H, Pfeffer R and Lynch G 1988 Olfactory testing as possible probes for detecting and monitoring Alzheimer's disease *Neurobiol. Aging* **9** 399–403

[4] DeToledo-Morrell L, Goncharova I, Dickerson B, Wilson R S and Bennet D A 2000 From healthy aging to early Alzheimer's disease: in vivo detection of entorhinal cortex atrophy *Ann. NY Acad. Sci.* **911** 240–53

[5] Devanand D P, Michaels-Marston K S, Liu X, Pelton G H, Padilla M, Marder K, Bell K, Stern Y and Mayeux R 2000 Olfactory deficits in patients with mild cognitive impairment predict Alzheimer's disease at follow-up *Am. J. Psychiatry* **157** 1399–405

[6] Murphy C, Gilmore M M, Seery C S, Salmon D P and Lasker B R 1990 Olfactory thresholds are associated with degree of dementia in Alzheimer's disease *Neurobiol. Aging* **11** 465–9

[7] Mesholam R I, Moberg P J, Mahr R N and Doty R L 1998 Olfaction in neurodegenerative disease: a meta-analysis of olfactory functioning in Alzheimer's and Parkinson's disease *Arch. Neurol.* **55** 84–90

[8] Hawkes C H and Shephard B C 1998 Olfactory evoked responses and identification tests in neurological disease *Ann. NY Acad. Sci.* **855** 608–15

[9] Hawkes C H, Shephard B C, Geddes J F, Body G C and Martin J E 1998 Olfactory disorder in motor neuron disease *Exptal. Neurol.* **150** 248–53

[10] Devanand D P, Michael-Marston M A, Liu X, Pelton G H, Padilla M, Marder K, Bell B, Stern Y and Mayeus R 2000 Olfactory deficits in patients with mild cognitive impairment predict Alzheimer's disease at follow-up *Am. J. Psychiatry.* **157** 1399–405

[11] Ponsen M M, Stoffers D, Booij J, van Eck-Smith B L, Wolters E Ch and Berendse H W 2004 Idiopathic hyposmia as a preclinical sign of Parkinson's disease *Ann. Neurol.* **56** 173–81

[12] Doty L 1997 Studies of human olfaction from the University of Pennsylvania Smell and Taste Center *Chem. Senses* **22** 565–86

[13] Doty R L, Gregor T P and Settle R G 1986 Influence of intertrial interval and sniff-bottle volume on phenyl ethyl alcohol odor detection thresholds *Chem. Senses* **11** 259–64

[14] Doty R L, Shamaan P, Kimmelenson C P and Dann M S 1984 University of Pennsylvania Smell Identification Test: a rapid quantitative olfactory test for the clinic *Laryngoscope* **94** 176–8

[15] Doty R L, Bromley S M and Stern M B 1995 Olfactory testing as an aid in the diagnosis of Parkinson's disease: development of optimal discrimination criteria *Neurodegen* **4** 93–7

[16] http://www.odotech.qc.ca/en/products/odile/specifications.html

[17] Walker J C, Kurtz D B, Shore F M, Ogden M W and Reynolds J H 1990 Apparatus for the automated measurement of the responses of humans to odorants *Chem. Senses* **15** 165–77

[18] Youngentob S L 2005 A method for the rapid automated assessment of olfactory function *Chem. Senses* **30** 219–29

[19] Hayes D J, Achiriloaie I, Taylor D W, Comparini N and Wallace D B 2002 Digital olfactometer and method for testing olfactory thresholds *US Patent* 6,338,715

[20] Frederickson C J, Wallace D B, Hayes D J, Taylor D W and Hayes M D 2002 Method and apparatus for delivery of fragrances and vapors to the nose *US Patent* 6,390,453

[21] Taylor D W and Achiriloaie I 2002 Cartridge element for micro jet dispensing *US Patent* 6,378,988

[22] Doty R L, Brugger W E, Jurs P C, Orndorff M A, Snyder P J and Lowry L D 1978 Intranasal trigeminal stimulation from odorous volatiles: psychometric responses from anosmic and normal humans *Physiol. Behav.* **20** 175–85

[23] Ruiz O and Black W Z 2002 Evaporation of Water Droplets Placed on Heated Horizontal surface *ASME J. Heat Transfer* **124** 854–63

[24] Holman J P 1986 *Heat Transfer* (New York: McGraw-Hill)

[25] Kurtz D B, Zhao K, Hornung D E and Scherer P 2004 Experimental and numerical determination of odorant solubility in nasal and olfactory mucosa *Chem. Senses* **29** 763–73

[26] Lotsch J, Nordin S, Hummel T, Murphy C and Kobal G 1997 Chronobiology of nasal chemosensitivity: do odor or trigeminal pain thresholds follow a circadian rhythm? *Chem. Senses* **22** 593–8

[27] Dyck P J, Karnes J L, Gillen D A, O'Brien P C, Zimmerman I R and Johnson D M 1990 Comparison of algorithms of testing for use in automated evaluation of sensation *Neurology* **40** 1607–13

[28] Hummel T, Guel H and Delank W 2004 Olfactory sensitivity of subjects working in odorous environments *Chem. Senses* **29** 533–6

[29] Folstein M, Folstein S and McHugh P R 1975 Mini-mental state: A practical method for grading the cognitive status of patients for the clinician *J. Psychol. Res.* **12** 189–98